Electronic Supplementary Information for

Constructing Sheet-Assembled Hollow CuSe Nanocubes to Boost the Rate Capability for Rechargeable Magnesium Batteries

Changliang Du,[a] Waqar Younas,[a] Zhitao Wang,[a] Xinyu Yang,[a] Erchao Meng,[b] Liqin Wang,[a] Jiaqin Huang,[a] Xilan Ma,[a] Youqi Zhu,*[a] Chuanbao Cao*[a]

[a.] Research Center of Materials Science, Beijing Key Laboratory of Construction Tailorable Advanced Functional Materials and Green Applications, Beijing Institute of Technology, Beijing 100081, China, E-mail: yqzhu@bit.edu.cn (Y. Zhu), cbcao@bit.edu.cn (C. Cao).

[b.] Henan Provincial Key Laboratory of Surface and Interface Science, Zhengzhou University of Light Industry, Zhengzhou 450001, China.

Experimental details

Preparation of the electrolyte

The $Mg(BH_4)_2/(CF_3)_2CHOH$/DME electrolyte was prepared in an argon-filled glove box followed by the previous works[S1, S2] after a minor revision. In a typical preparation, 0.10 g $Mg(BH_4)_2$ (95%, Sigma Aldrich) were dispersed in 7 mL DME (99.0%, Alfa Asear) under continuous stirring to obtain a clear solution. Afterwards, 1.6 mL hexafluoroisopropanol ($(CF_3)_2CHOH$, 99%, Aladdin) were dropwise added in above solution under stirring. The solution was stirred and dried at room temperature for about 4 days to obtain a solid state. Finally, 6 mL DME is added to the dissolved solids to obtain the 0.3 M $Mg(BH_4)_2$/DME electrolyte.

The $(Mg(HMDS)_2)$-$AlCl_3$/DME electrolyte and $Mg(AlCl_2EtBu)_2$/THF electrolyte were prepared according to our previous works.[S3, S4]

Synthesize of the CuSe NPs

The CuSe NPs were prepared with the high-temperature microwave-assisted method followed by the published work.[S5] In a typical preparation, 1 mmol $Cu(CH_3COOH)\cdot H_2O$ and 1 mmol Na_2SeO_3 were dispersed in 50 mL distilled water by stirring for 30 min. Afterwards, 1 mL 80% hydrazine hydrate and 2 mL ammonium hydroxide were dropwise added in above solution. And then the mixed solution was transformed to a 250 mL flask and put into a microwave reactor at 105℃ for 15 min at 400 W. The products were collected and washed centrifugally with ethanol and distilled water for several times. Finally, the CuSe NPs were obtained after dried at 80℃ overnight.

Supplementary figures and tables

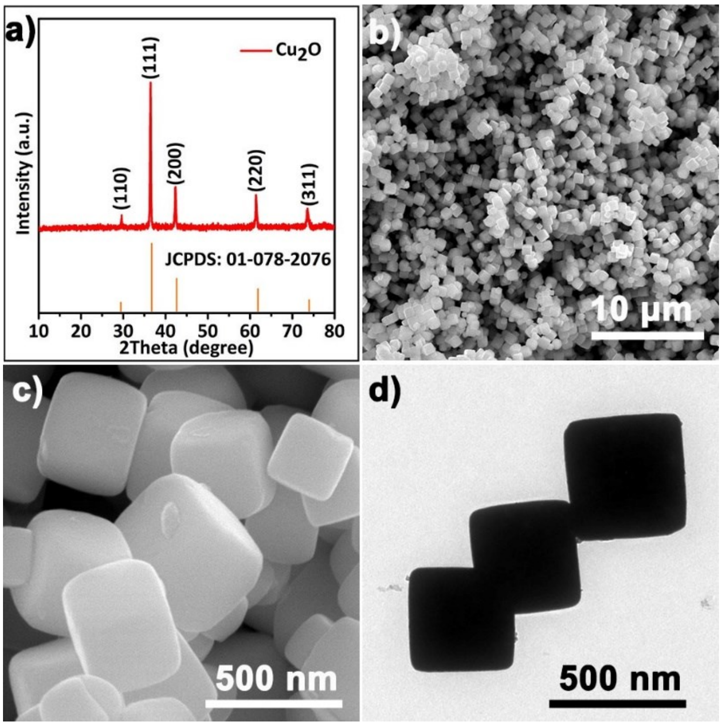

Figure S1. (a) XRD pattern, (b) low-magnification SEM image, (c) high-magnification image and (d) TEM image of the precursor Cu_2O solid cubes.

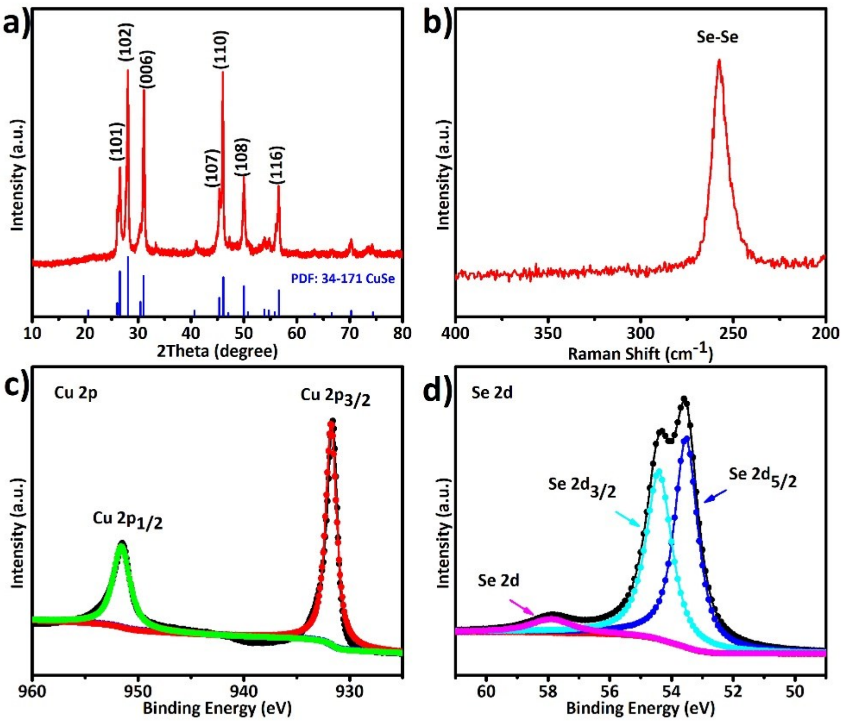

Figure S2. (a) XRD pattern, (b) Raman spectrum, and XPS spectra of (c) Cu 2p and (d) Se 3d of CuSe NPs.

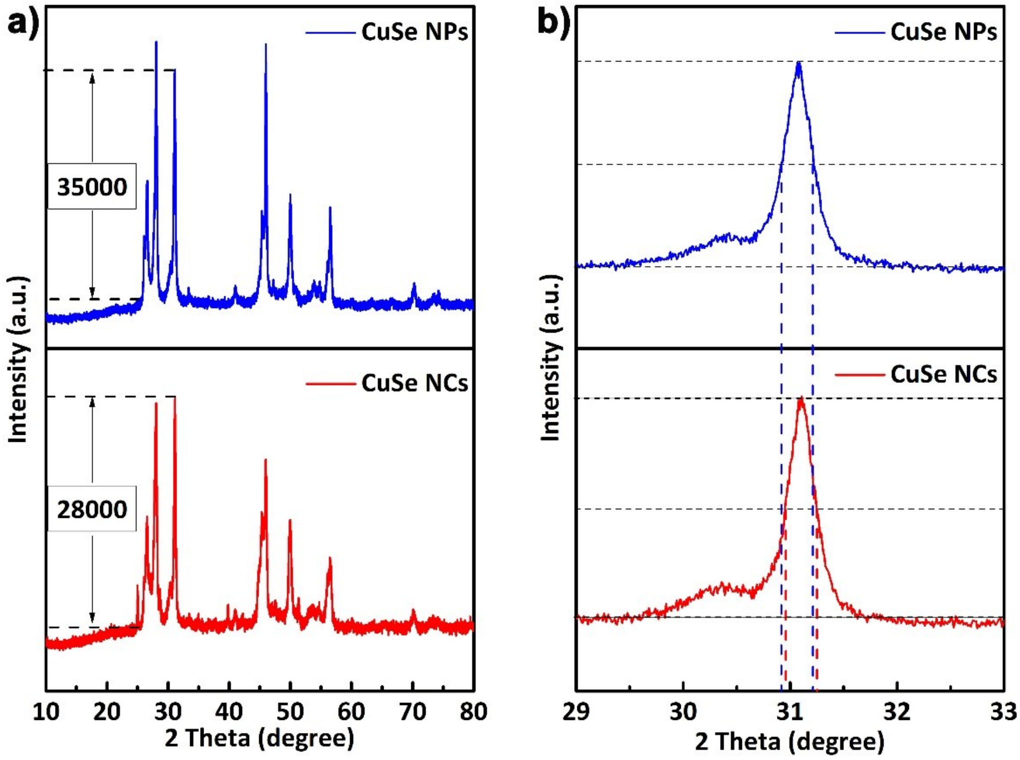

Figure S3. (a, b) XRD patterns of CuSe NCs and CuSe NPs.

The similar peak intensity and half-peak width of the (006) plane diffraction of the CuSe NCs (prepared at room temperature) and CuSe NPs (prepared at 100℃) suggest a similar crystallinity of these two samples. In general, high temperature is more favorable for obtaining samples with good lattice arrangement. Therefore, we believe that the good crystallization of CuSe NCs prepared at room temperature can be attributed to the highly active selenide solution used.

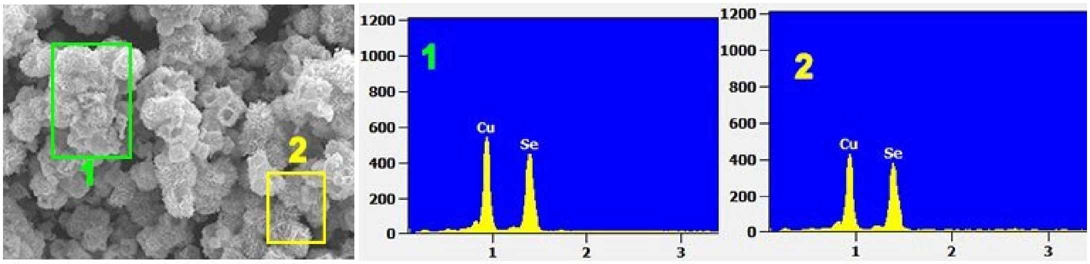

	Cu-L	Se-L
1	53.47	46.53
2	53.79	46.21

Figure S4. EDX results of CuSe NCs and corresponding ratio of elements to components.

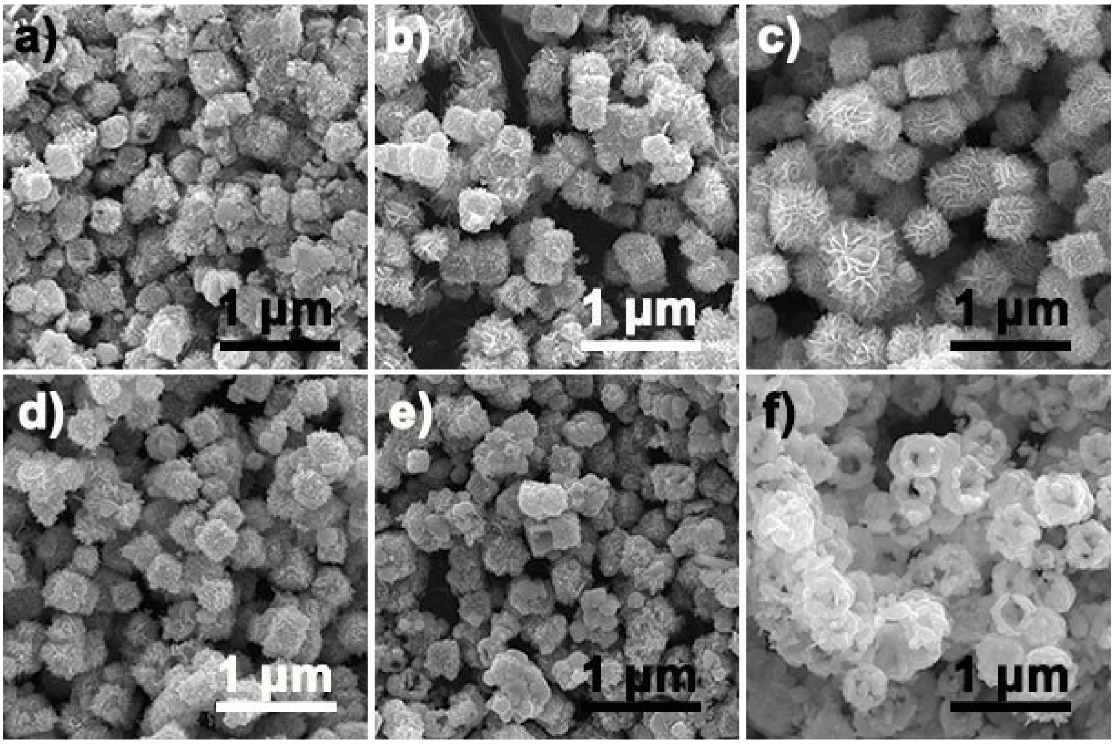

Figure S5. SEM images of the CuSe NCs during different selenide time of (a) 5min, (b) 10 min, (c) 15 min, (d) 20 min, (e) 30 min and (f) 60 min.

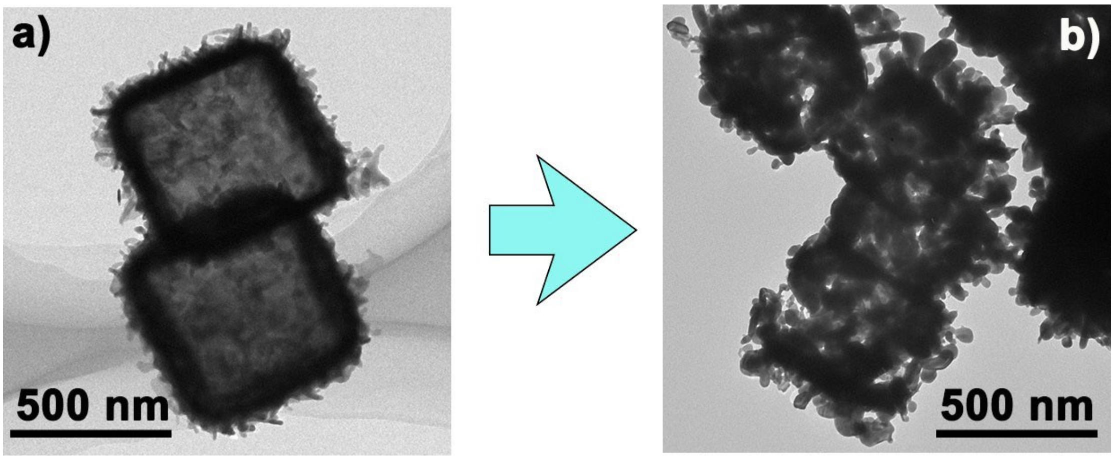

Figure S6. TEM images of CuSe NCs at different selenide time of (a) 15 min and (b) 60 min.

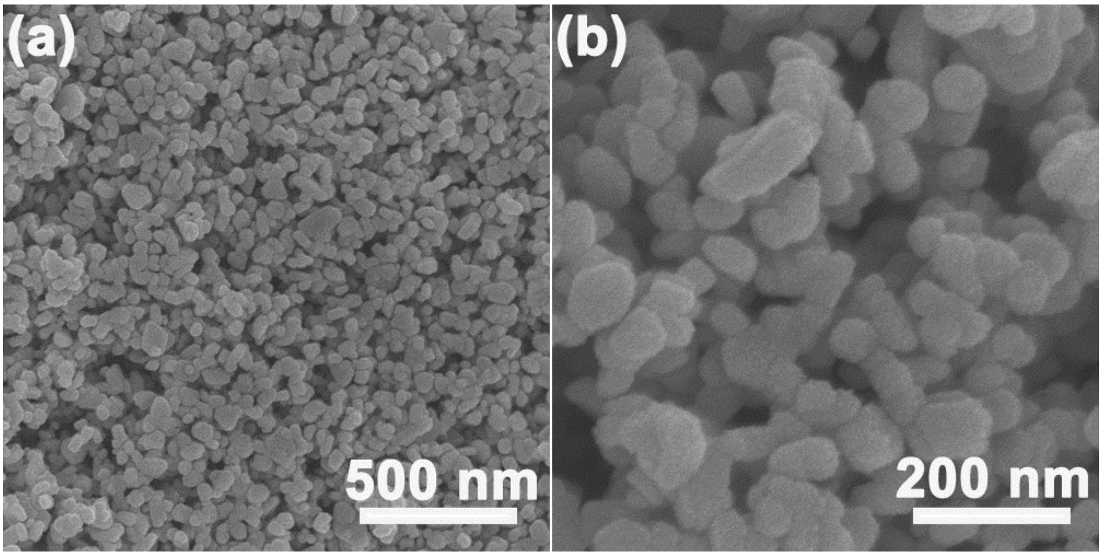

Figure S7. (a) low- magnification and (b) high-magnification SEM images of the CuSe NPs.

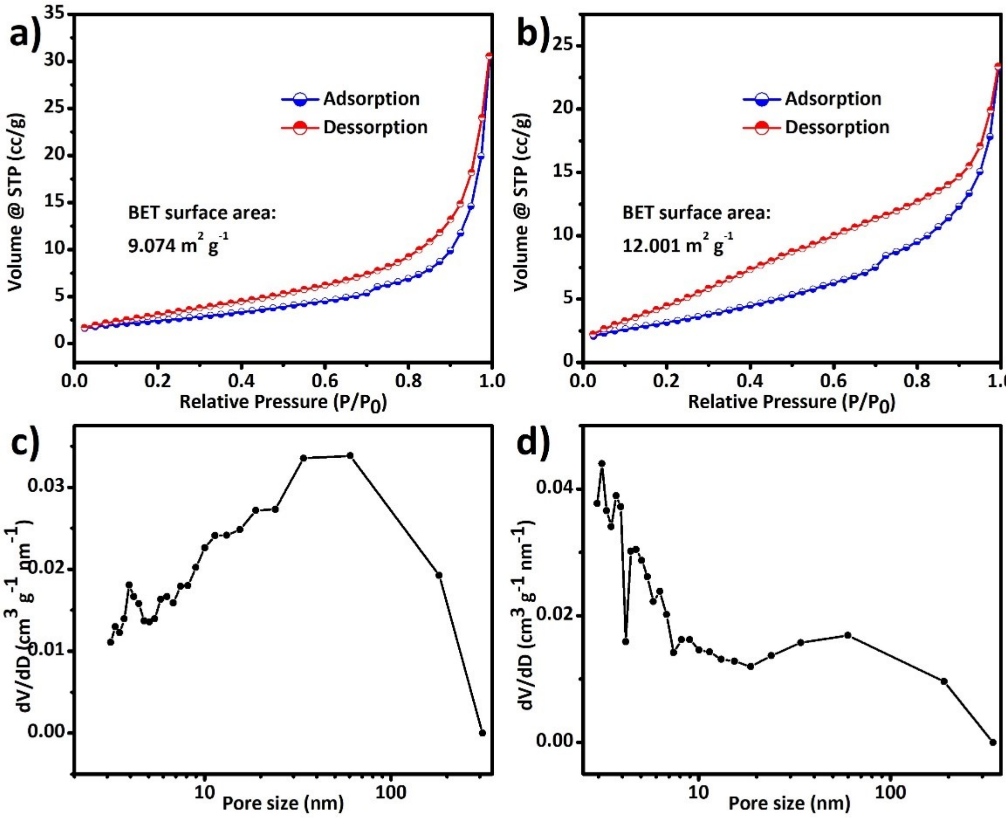

Figure S8. N_2 adsorption–desorption pattern and of (a) CuSe NCs, (b) CuSe NPs, and BJH pore size distribution of (c) CuSe NCs, (d) CuSe NPs.

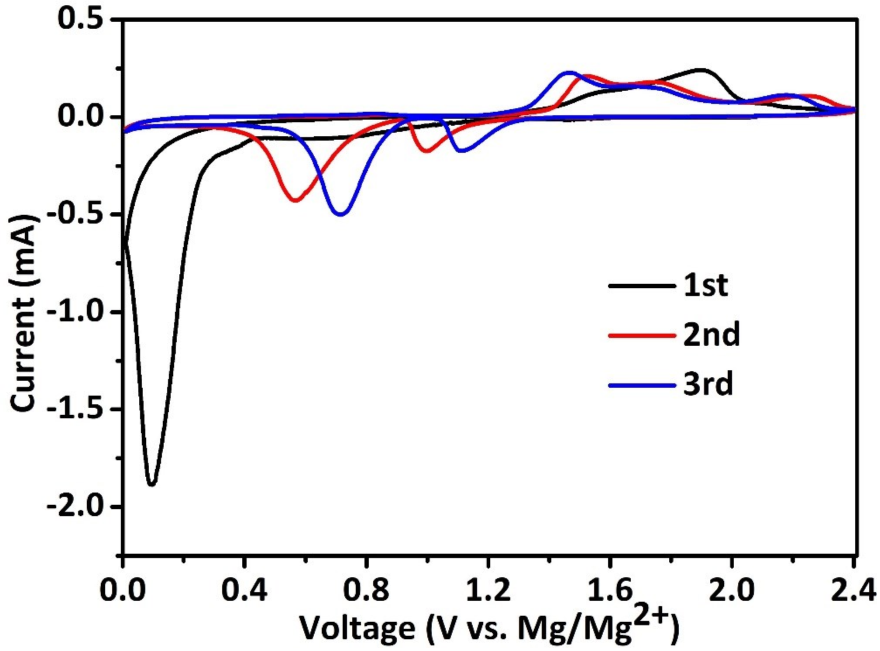

Figure S9. CV curves of the fresh CuSe NCs electrode in $Mg(BH_4)_2/(CF_3)_2CHOH/DME$ electrolyte before activated process.

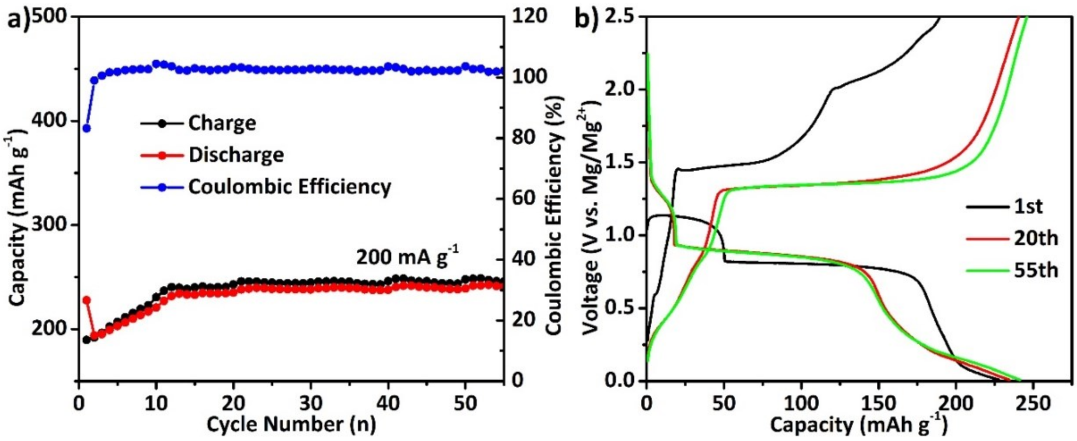

Figure S10. a) Cycling performance, b) charge-discharge voltage profiles of CuSe NCs electrode at 200 mA g^{-1} in the voltage window of 0.01-2.5 V.

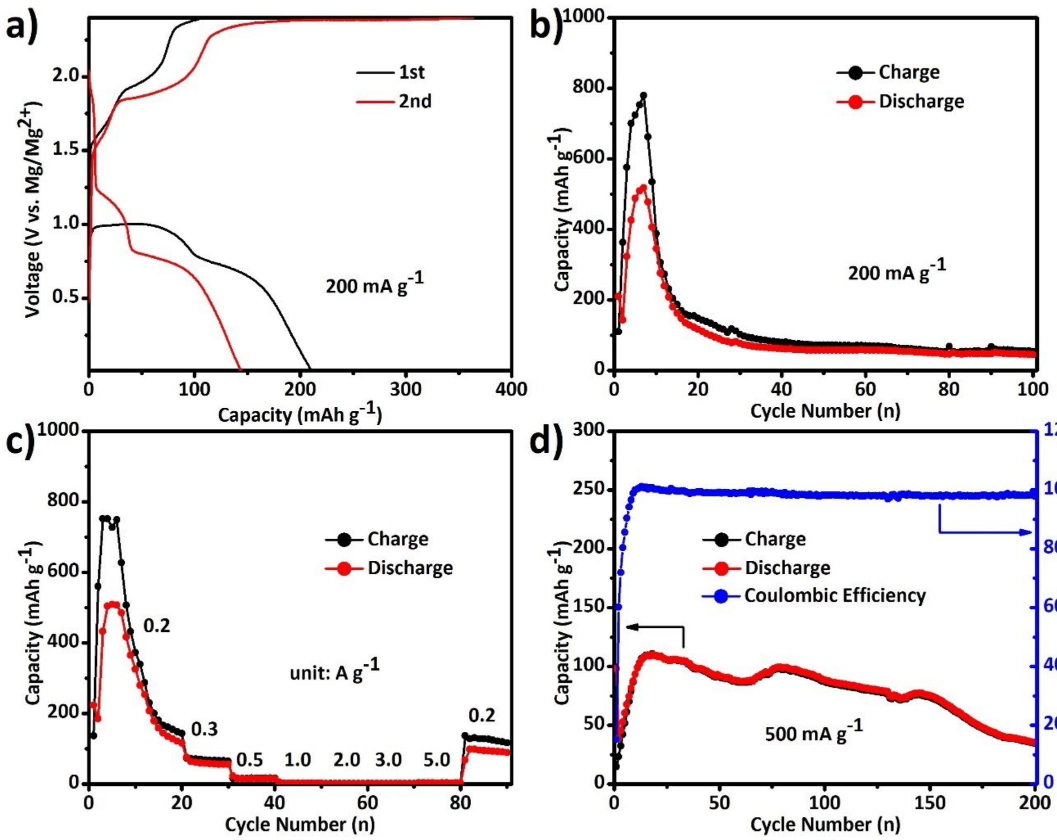

Figure S11. Electrochemical magnesium storage performance of CuSe NCs cathode in $Mg(AlCl_2EtBu)_2$/THF electrolyte: (a) charge-discharge voltage profiles at 200 mA g^{-1}, (b) cycling performance at 200 mA g^{-1}, (c) rate capability and (d) cycling property at 500 mA g^{-1}.

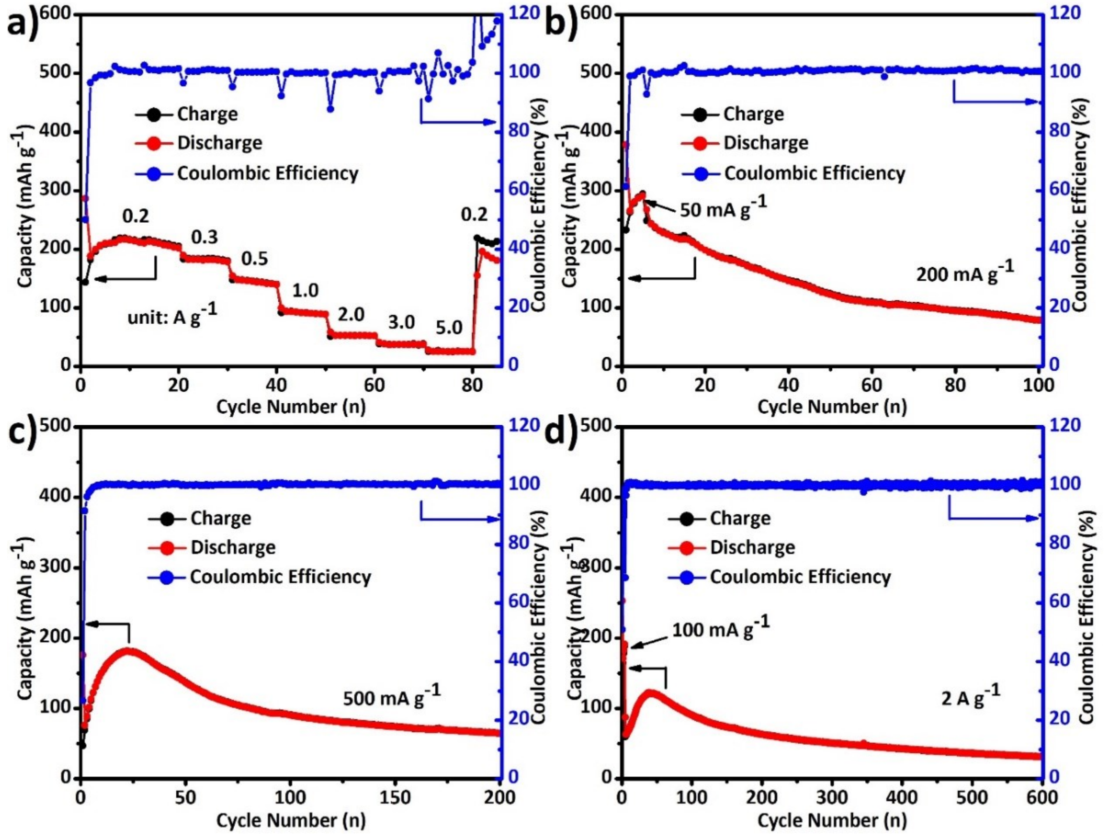

Figure S12. Electrochemical magnesium storage properties of CuSe NCs electrode in (Mg(HMDS)$_2$)-$AlCl_3$/DME electrolyte: (a) rate property, cycling performances at (b) 200 mA g^{-1}, (c) 500 mA g^{-1} and (d) 2 A g^{-1}.

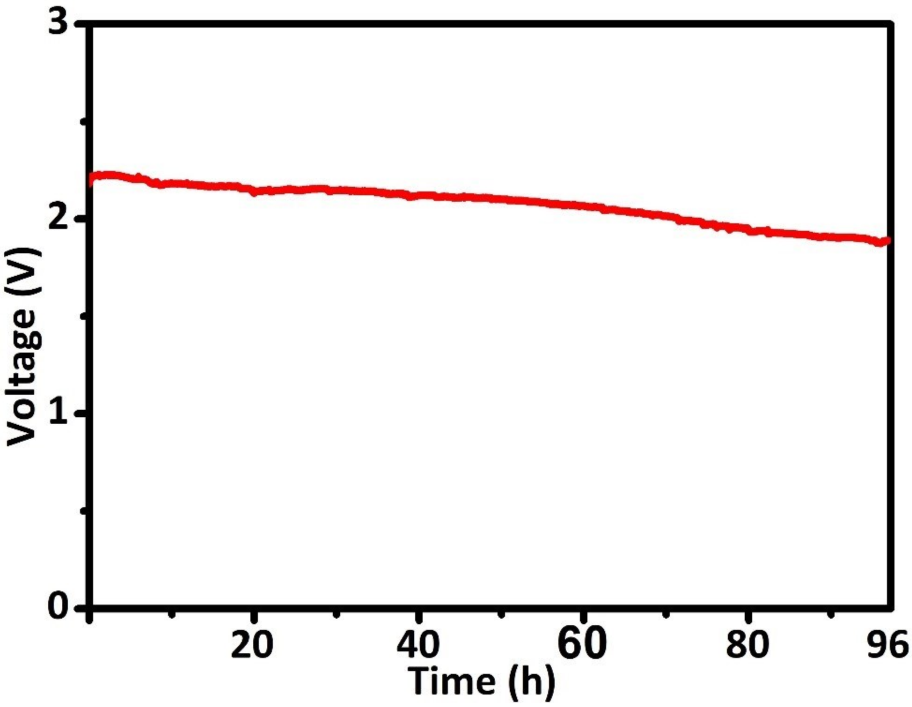

Figure S13. The open-circuit voltage during open circuits of 96 h to investigate the self-discharge behavior of the cells assembled with CuSe NCs cathode and $Mg(BH_4)_2/(CF_3)_2CHOH/DME$ electrolyte.

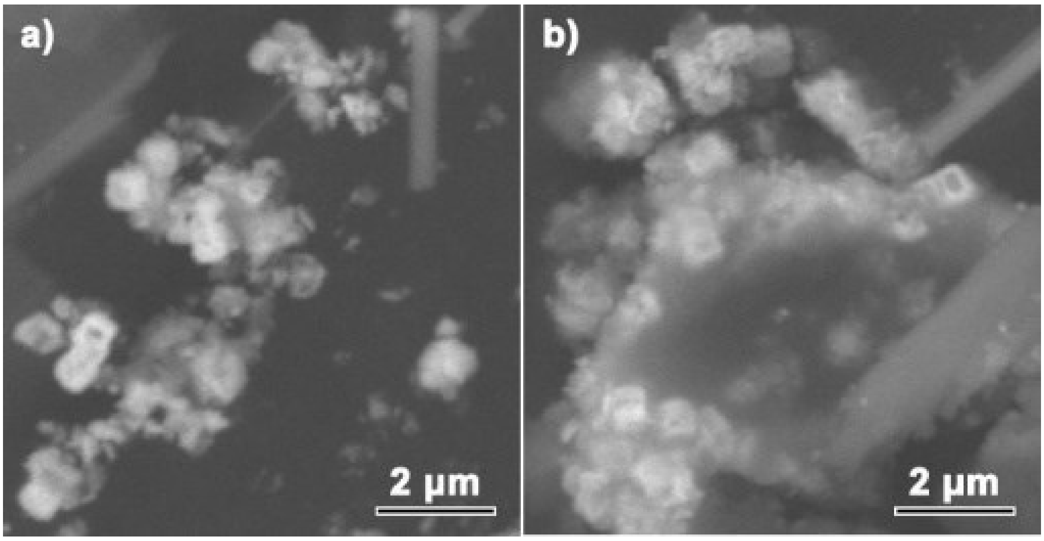

Figure S14. (a, b) SEM images of the CuSe NCs electrode after prolonged cycling.

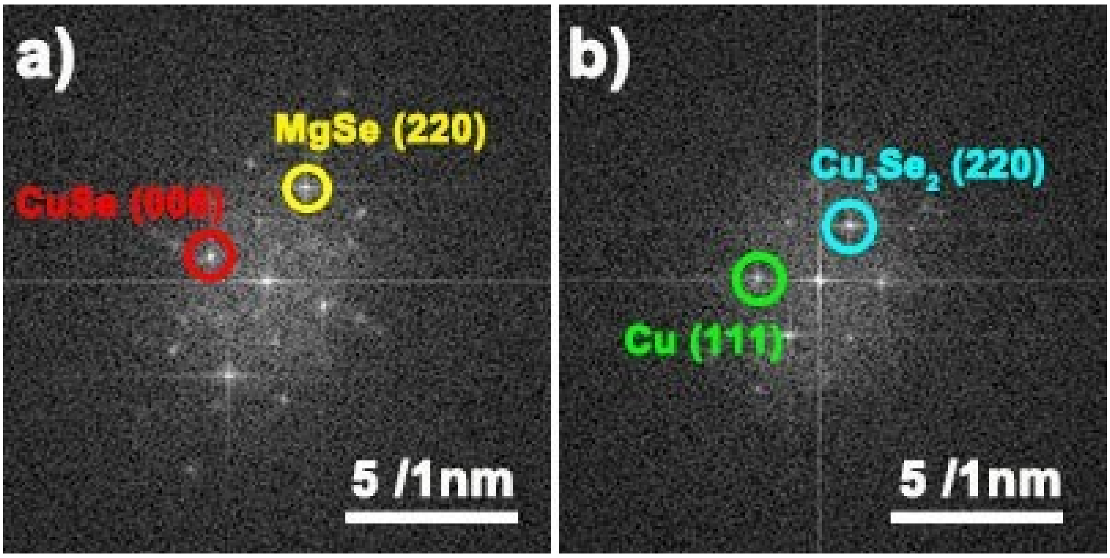

Figure S15. (a, b) Fast Fourier transform electron diffraction pattern of the fully discharged cathode.

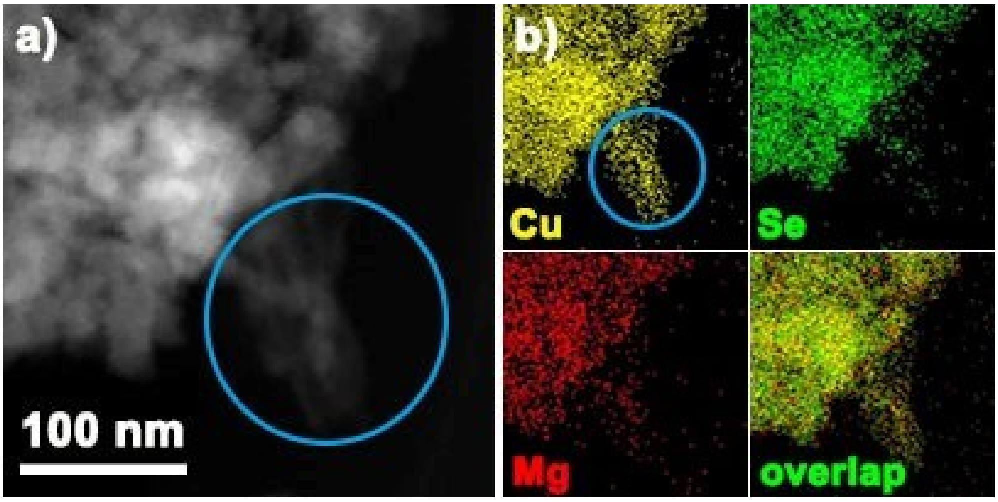

Figure S16. (a) STEM image and (b) corresponding EDS elemental mapping at the fully discharged state

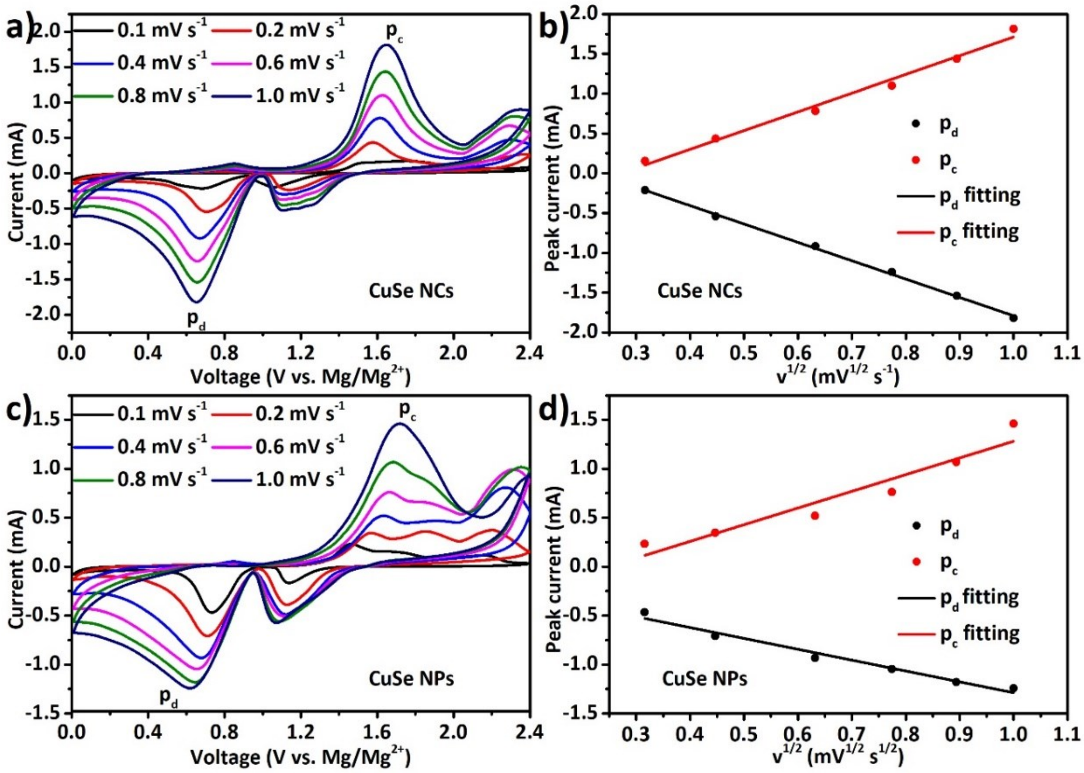

Figure S17. CV tests and plots of CV peak current at various scan rates. CV curves and peak currents versus square root of scan rates of (a, b) the CuSe NCs and (c, d) CuSe NPs electrodes.

Table S1. Summary about the Mg storage properties of some related electrode materials

Cathode Materials	**Voltage Window (V vs. Mg/Mg^{2+})**	**Current Density (mA g^{-1})**	**Capacity (mAh g^{-1})**	**Reference**
CuS	0.01-2.4	50	477	S1
		1000	90	
$CuS_{1-x}Se_x$ NSs	0-2.0	20	268.5	S3
		500	119.2	
CuS NSs	0-2.0	20	400	S4
		200	200	
CuSe NPs	0.2-2.0	10	203	S5
		100	50	
CuS NCs	0.1-2.4	100	200	S6
		1000	50	
Cu_3Se_2	0.1-2.0	100	277	S7
		1000	245	
CuSe NCs	0.3-2.2	100	250	S8
		1000	60	
R-$CoSe_2$	0-2.5	50	210	S9
		1000	70	
NaV_6O_{15}	1.6-2.9	10	210.1	S10
		500	27.2	
V_2O_5	0.1-2.0	50	120	S11
		200	62	
CoS	0.1-2.0	50	125	S12
		150	90	
Mo_6S_8	0.5-1.8	12	110	S13
		600	78	
CuSe nanocubes	0.01-2.4	200	254.4	This work
		5000	77.6	

Notes and references

S1. Y. Shen, Y. Wang, Y. Miao, M.Yang, X. Zhao, X. Shen, *Adv. Mater.* **2019**, 12, 1905524.

S2. Z. Z. Karger, M. E. G. Bardaji, O. Fuhr, M. Fichtner, *J. Mater. Chem. A.* **2017**, 5, 10815-10820

S3. Z. Wang, Y. Zhu, C. Qiao, S. Yang, J. Jia, S. Rafai, X. Ma, S. Wu, F. Ji, C. Cao, *Small*, **2019**, 15, 1902797.

S4. Z. Wang, S. Rafai, C. Qiao, J. Jia, Y. Zhu, X. Ma, C. Cao, *ACS Appl. Mater. Interfaces*, **2019**, 11, 7046−7054.

S5. S. Yang, F. Ji, Z. Wang, Y. Zhu, K. Hu, Y. Ouyang, R. Wang, X. Ma, C. Cao, *Electrochim. Acta,* **2019**, 324, 134864.

S6. J. Shen, Y. Zhang, D. Chen, X. Li, Z. Chen, S. Cao, T. Li, F. Xu, *J. Mater. Chem. A.* **2019**, 7, 21410−21420.

S7. X. Cheng, Z. Zhang, Q. Kong, Q. Zhang, T. Wang, S. Dong, L. Gu, X. Wang, J. Ma, P. Han, H. Lin, C. Chen, G. Cui, *Angew. Chem. Int. Ed.* **2020**, 59, 11477−11482.

S8. J. Shen, D. Chen, S. Cao, T. Li, W. Luo, F. Xu, *Dalton Trans.* **2020**, 49, 13253−13261.

S9. D. Chen, Y. Zhang, X. Li, J. Shen, Z. Chen, S. Cao, T. Li, F. Xu, *Nanoscale,* **2019**, 11, 23173−23181.

S10. D. Wu, J. Zeng, H. Hua, J. Wu, Y. Yang, J. Zhao, *Nano Res*. **2020**, 13, 335−343.

S11. Y. Xiao, M. Pan, J. Zou, R. Guo, X. Zeng, W. Ding, *Ionics,* **2019**, 25, 5889−5897.

S12. D. He, D. Wu, J. Gao, X. Wu, X. Zeng, W. Ding, *J. Power. Sources,* **2015**, 294, 643−649.

S13. M. Mao, Z. Lin, Y. Tong, J. Yue, C. Zhao, J. Lu, Q. Zhang, L. Gu, L. Suo, Y. Hu, H. Li, X. Huang, L. Chen, *ACS Nano*, **2020**, 14, 1102−1110.